Singular Plastic Fields in Steady Penetration of a Rigid Cone

David Durban
Faculty of Aerospace Engineering,
Technion—Israel Institute of Technology,
Haifa 32000, Israel

Norman A. Fleck
Department of Engineering,
Cambridge University,
Cambridge CB2 1PZ, U.K.

The essential features of the active plastic zone at the tip of a penetrating rigid cone are investigated for a rigid/perfectly plastic solid. An exact solution is suggested for the plastic zone. A rigid zone exists ahead of the cone and is separated from the plastic zone by a conical surface of discontinuity. It is assumed that the material yields instantaneously by going through a "shear shock" across the rigid/plastic interface. The orientation of the interface is determined by an ad hoc requirement for minimum shear strain jump at the shear shock. Results are presented for different cone angles and friction factors. The stresses within the plastic zone admit a logarithmic singularity whose level increases with cone angle and wall friction.

Introduction

Local singular fields at the tip of a rigid conical indentor, penetrating an incompressible power-law viscous solid have been studied recently by Fleck and Durban (1990). The limiting case of that analysis for vanishing strain-rate exponent describes possible singular fields of rigid/perfectly plastic materials with logarithmic singularity of the stresses and a power-type strain rate singularity. The plastic zone of this solution extends continuously over the entire near-tip volume of the penetrated solid.

In the present paper we address the problem of rigid/perfectly plastic singular fields, near a tip of a penetrating cone, employing an alternative model. It is thought that the new solution is relevant to surface indentation and to deep penetration by a rigid cone. Following existing studies on discontinuous rigid/plastic conical fields (Lockett, 1963; Shield, 1955; Spencer, 1984) we assume that the material ahead of the cone remains rigid up to a rigid/plastic interface (Fig. 1). At that conically shaped interface, the solid yields instantaneously by passing through a "shear shock." The mathematical model is constructed in the spirit of earlier studies of orthogonal machining, where rigid/perfectly plastic theory gives useful physical insight to the problem. In particular, machining theory suggests a shear shock at an angle which bisects the machining direction and the angle of the tool face. This prediction is borne out by experimental observation (Johnson and Mellor, 1973). The rigid/plastic interface simulates a more diffuse transition zone where the streamlines possess high local curvature.

An exact, almost closed-form solution is suggested for the active plastic zone which extends from the interface to the cone. Surface roughness is accounted for by imposing a friction factor along the wall. The shear stress $\sigma_{r\theta}$ on the wall is given by $|\sigma_{r\theta}| = mk$ where k is the shear yield stress and the friction factor m ranges from zero to unity. The stresses have a logarithmic singularity while the strain rates singularity is r^{-1}. The latter is stronger than the strain rate singularities reported earlier by Fleck and Durban (1990). A similar conclusion holds for the level (amplitude) of the logarithmic stress singularity. More refined boundary value calculations are required in order to assess which of the two solutions is the more frequently encountered in penetration and indentation problems.

At the rigid/plastic interface we impose a pragmatic ad hoc requirement that the finite jump in the shear strain attains its smallest possible value. This condition determines uniquely the shear shock orientation, approximately in a direction bisecting the angle between the cone's wall and the penetrating axis.

Detailed results are presented for the influence of cone angle and wall friction on the interface orientation, the shear strain jump at the interface, level of stress singularity, and shape of streamlines. The paper concludes with a brief discussion of Spencer's (1984) model, which is here recovered as a special case for one particular cone angle and friction condition.

We assume a von Mises yield law and an associated flow rule, while previous studies (Lockett, 1963; Shield, 1955; Spencer, 1984) employ a Tresca yield law. The present analysis

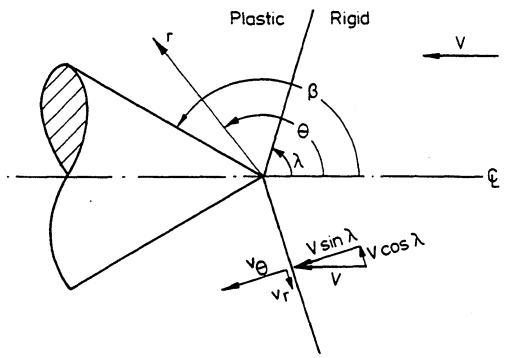

Fig. 1 Convention for steady penetration of a rigid cone. A "shear shock" discontinuity at $\theta = \lambda$ marks the rigid/plastic interface.

Contributed by the Applied Mechanics Division of THE AMERICAN SOCIETY OF MECHANICAL ENGINEERS for publication in the ASME JOURNAL OF APPLIED MECHANICS.

Discussion on this paper should be submitted to the Technical Editor, Prof. Leon M. Keer, The Technological Institute, Northwestern University, Evanston, IL 60208, and will be accepted until four months after final publication of the paper itself in the ASME JOURNAL OF APPLIED MECHANICS.

Manuscript received by the ASME Applied Mechanics Division, Sept. 24, 1990; final revision, July 22, 1991. Associate Technical Editor: J. W. Rudnicki.

provides, apparently for the first time, an analytical solution for the velocities and stresses within the singular plastic zone. This enables us to examine the details of the coupling between wall friction and cone angle.

Field Equations and Solution

We consider a rigid cone that penetrates a rigid/perfectly plastic solid (Fig. 1). Assume low velocity steady-state conditions and concentrate on the near-tip singular field. An Eulerian frame of reference is attached to the apex with spherical coordinates (r, θ, ϕ). Material behavior is modeled as rigid ahead of the cone, up to an instantaneous shear surface at $\theta = \lambda$, and as perfectly plastic within the region bounded by the rigid/plastic interface and the cone's wall at $\theta = \beta$.

The constitutive relation in the plastic sector is given by

$$\mathbf{S} = \sqrt{\frac{2}{3}}\,\sigma_o \frac{\mathbf{D}}{\sqrt{\mathbf{D}\cdot\cdot\mathbf{D}}} \tag{1}$$

where $\mathbf{S}$ is the stress deviator tensor, $\mathbf{D}$ is the Eulerian strain rate tensor, and σ_o is the yield stress in simple tension. Assuming that the velocity field depends only on θ, we find that material incompressibility of (1) is maintained if the velocities are expressed as (Fleck and Durban, 1990)

$$v_r = \phi' + \phi\cot\theta \tag{2}$$

$$v_\theta = -2\phi \tag{3}$$

where (v_r, v_θ) denote the (r, θ) velocity components, ϕ is a velocity potential that depends only on θ, and $(\,)' \equiv d(\,)/d\theta$.

The strain rate components follow from (2)–(3) in the form

$$\epsilon_{rr} = 0 \tag{4}$$

$$\epsilon_{\theta\theta} = -\epsilon_{\phi\phi} = -\frac{1}{r}\,(\phi' - \phi\cot\theta) \tag{5}$$

$$\epsilon_{r\theta} = \frac{1}{2r}\,[(\phi' + \phi\cot\theta)' + 2\phi]. \tag{6}$$

Inserting relations (4)–(6) in (1) we obtain the deviatoric components

$$\sigma_{rr} - \sigma_h = 0 \tag{7}$$

$$\sigma_{\theta\theta} - \sigma_h = -(\sigma_{\phi\phi} - \sigma_h) = -k\,\frac{\phi' - \phi\cot\theta}{\Gamma} \tag{8}$$

$$\sigma_{r\theta} = k\,\frac{Y}{\Gamma} \tag{9}$$

where σ_h is the hydrostatic stress,

$$Y = \frac{1}{2}\,[(\phi' + \phi\cot\theta)' + 2\phi] \tag{10}$$

$$\Gamma^2 = Y^2 + (\phi' - \phi\cot\theta)^2, \tag{11}$$

and $k = \sigma_o/\sqrt{3}$ is the shear yield stress. Notice that $\Gamma(\theta)$ gives the angular dependence of the effective strain rate $\epsilon_{\text{eff}} = (2/3\,\mathbf{D}\cdot\cdot\mathbf{D})^{1/2} \equiv 2\Gamma/\sqrt{3}r$.

Since the state of stress is axially symmetric, there are just two equations of equilibrium, namely

$$r\sigma_{rr,r} + 2\sigma_{rr} - \sigma_{\theta\theta} - \sigma_{\phi\phi} + \sigma_{r\theta,\theta} + \sigma_{r\theta}\cot\theta = 0 \tag{12}$$

$$r\sigma_{r\theta,r} + 3\sigma_{r\theta} + \sigma_{\theta\theta,\theta} + (\sigma_{\theta\theta} - \sigma_{\phi\phi})\cot\theta = 0. \tag{13}$$

On substituting the stresses from (7)–(9) into the radial Eq. (12), we find that the hydrostatic stress must be of the form

$$\sigma_h = k[H(\theta) + D\ln r] \tag{14}$$

where D is a constant and $H(\theta)$ is an unknown function of θ. It follows that radial equilibrium is maintained if

$$Y' - Y\frac{\Gamma'}{\Gamma} + Y\cot\theta + D\Gamma = 0 \tag{15}$$

or, after one integration,

$$Y = F(\theta)\Gamma \tag{16}$$

with

$$F = \frac{D\cos\theta + F}{\sin\theta} \tag{17}$$

where E is an integration constant. Combining (16) with (11), and observing that both Γ and $\epsilon_{\phi\phi}$ are positive, gives

$$Y = \frac{F}{\sqrt{1 - F^2}}\,(\phi' - \phi\cot\theta). \tag{18}$$

Now eliminate Y between (18) and (10). We arrive at the linear differential equation

$$\phi'' + \left(\cot\theta - \frac{2F}{\sqrt{1-F^2}}\right)\phi' + \left(2 - \frac{1}{\sin^2\theta} + \frac{2F}{\sqrt{1-F^2}}\cot\theta\right)\phi = 0. \tag{19}$$

This equation admits the solution

$$\phi = C_1\sin\theta + C_2 f(\theta)\sin\theta \tag{20}$$

where

$$f(\theta) = \int_\lambda^\theta \frac{g(\theta)}{\sin^3\theta}\,d\theta \tag{21}$$

$$g(\theta) = \exp\int_\lambda^\theta \frac{2F}{\sqrt{1-F^2}}\,d\theta \tag{22}$$

and C_1, C_2 are integration constants.

It still remains to solve the second equation of equilibrium (13); substituting the stresses (7)–(9) and (14) into (13) results in

$$H' = (\sqrt{1-F^2})' + 2\sqrt{1-F^2}\cot\theta - 3F. \tag{23}$$

The integral of (23), obtained with the aid of (17), completes the solution of the equilibrium equations. It is worth noting that the deviatoric components (7)–(9) may be rewritten, by (16) and (18), as

$$\sigma_{rr} - \sigma_h = 0 \tag{24}$$

$$\sigma_{\theta\theta} - \sigma_h = -(\sigma_{\phi\phi} - \sigma_h) = k\sqrt{1-F^2} \tag{25}$$

$$\sigma_{r\theta} = kF. \tag{26}$$

Function F determines the relative contribution of the shear stress to the overall yield stress k.

Boundary Conditions

Turning to the boundary conditions and assuming a maximum shear rigid/plastic interface, we have that $\sigma_{r\theta} = k$ at $\theta = \lambda$ or, from (26),

$$F(\lambda) = 1. \tag{27}$$

Wall friction on the penetrating cone is represented by a shear factor m which controls the level of resisting shear stress at $\theta = \beta$ according to the relation $\sigma_{r\theta} = -mk$. Thus, from (26),

$$F(\beta) = -m. \tag{28}$$

The value of m ranges from $m = 0$ at a smooth wall to $m = 1$ at a perfectly rough wall. Combining conditions (27)–(28) with (17) gives

$$D = \frac{\sin\lambda + m\sin\beta}{\cos\lambda - \cos\beta} \tag{29}$$

$$E = -\frac{\sin\lambda\cos\beta + m\cos\lambda\sin\beta}{\cos\lambda - \cos\beta}. \tag{30}$$

The "shear-shock" at the rigid/plastic interface is supposed to simulate the narrow elastic-plastic transition zone which is expected to develop near $\theta = \lambda$. This model is constructed in the spirit of early studies on plane-strain machining (Johnson and Mellor, 1973) based on the maximum shear plane hypothesis. In reality, one may expect a relatively large curvature of the streamlines in the vicinity of the idealized shear shock.

The velocity potential (20) contains two constants (C_1, C_2) that can be determined from kinematical conditions. Denoting by V the uniform velocity of the rigid zone, relative to the cone, we have the condition of continuity of velocity normal to the interface (Fig. 1)

$$v_\theta(\lambda) = V\sin\lambda. \tag{31}$$

Along the wall, at $\theta = \beta$, v_θ has to vanish

$$v_\theta(\beta) = 0. \tag{32}$$

Both conditions (31)-(32) involve only the tangential velocity (3) which can be written, by (20), as

$$v_\theta = -2C_1\sin\theta - 2C_2 f(\theta)\sin\theta. \tag{33}$$

Inserting (33) in (31)-(32) we find

$$C_1 = -\frac{V}{2} \quad C_2 = \frac{V}{2f(\beta)}. \tag{34}$$

The interface angle λ is still undetermined. To this end we introduce the ad hoc requirement that the instantaneous shear strain at the interface will be as small as possible. The radial velocity jump at the interface is given by (Fig. 1).

$$\Delta v_r = v_r(\lambda) - (-V\cos\lambda). \tag{35}$$

From (2) and (20) we get the radial velocity component

$$v_r = 2C_1\cos\theta + 2C_2 f(\theta)\cos\theta + C_2\frac{g(\theta)}{\sin^2\theta}. \tag{36}$$

On substituting (36) in (35), observing that $f(\lambda) = 0$ and $g(\lambda) = 1$, and using (34), the velocity jump is

$$\Delta v_r = \frac{V}{2f(\beta)\sin^2\lambda}. \tag{37}$$

A measure of shear strain $\tan\gamma$ at the interface is therefore

$$\tan\gamma = \frac{\Delta v_r}{V\sin\lambda} = \frac{1}{2f(\beta)\sin^3\lambda} \tag{38}$$

where γ is the shear angle. We minimize (38) with respect to λ, for given values of β and m, in order to determine the orientation of the interface.

The strain rate components (4)-(6) may be put in the form

$$\epsilon_{rr} = 0, \quad \epsilon_{\theta\theta} = -\epsilon_{\phi\phi} = -\frac{1}{r}\left(\frac{V}{2f(\beta)}\right)\frac{g(\theta)}{\sin^2\theta}$$

$$\epsilon_{r\theta} = \frac{1}{r}\frac{F}{\sqrt{1-F^2}}\left(\frac{V}{2f(\beta)}\right)\frac{g(\theta)}{\sin^2\theta}.$$

At the rigid/plastic interface the normal components are simplified further, by (37), to

$$\epsilon_{\theta\theta} = -\epsilon_{\phi\phi} = -\frac{\Delta v_r}{r}.$$

Clearly, the shear strain rate component becomes unbounded at the interface where $F = 1$, and also at the wall when the friction factor m attains its highest value. The behavior of $\epsilon_{r\theta}$ near $\theta = \lambda$ is governed by

$$\epsilon_{r\theta} \sim \frac{\sqrt{2}\Delta v_r}{2\sqrt{D+\cot\lambda}}\cdot\frac{1}{r\sqrt{\theta-\lambda}}.$$

A similar expansion holds near the wall ($\theta = \beta$) when $m = 1$.

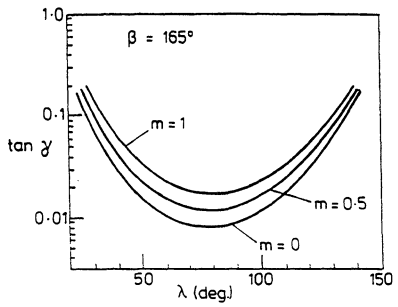

Fig. 2 Variation of shear strain with interface angle for different friction factors m. β = 165 deg.

Numerical Results and Discussion

The variation of the shear strain $\tan\gamma$ with interface angle λ, as evaluated from (38), is illustrated in Fig. 2 for a cone angle of 30 deg and with different values of m. As expected, there exists a clear minimum for the shear strain at a certain value of λ. That value of λ is taken here as the optimal orientation of the rigid/plastic interface within the framework of our model.

The numerical calculation of (38) involves the integrals (21)-(22); at the interface $F = 1$, by (27), and the integrand of (22) becomes unbounded. However, a straightforward expansion shows, with the aid of (17) and (29)-(30), that near $\theta = \lambda$

$$\int_\lambda^{\lambda+\Delta\theta}\frac{2F}{\sqrt{1-F^2}}\,d\theta \sim \frac{2\sqrt{2}}{\sqrt{A}}\sqrt{\Delta\theta} \quad \Delta\theta \ll 1 \tag{39}$$

where

$$A = \frac{1 + m\sin\lambda\sin\beta - \cos\lambda\cos\beta}{(\cos\lambda - \cos\beta)\sin\lambda}. \tag{40}$$

Similarly, when the wall is perfectly rough ($m = 1$) we have, near $\theta = \beta$, the expansion

$$\int_{\beta-\Delta\theta}^{\beta}\frac{2F}{\sqrt{1-F^2}}\,d\theta \sim -\frac{2\sqrt{2}}{\sqrt{B}}\sqrt{\Delta\theta} \quad \Delta\theta \ll 1 \tag{41}$$

with

$$B = \frac{\cos(\beta-\lambda) - \cos 2\beta}{(\cos\lambda - \cos\beta)\sin\beta}. \tag{42}$$

Expansions (39) and (41) have been used to overcome the numerical difficulties near $\theta = \lambda$, and near $\theta = \beta$ when $m = 1$.

The optimal location of the interface varies almost linearly with the angle β but shows little sensitivity to wall friction (Fig. 3). A rough approximation for the interface angle would be $\lambda \approx \beta/2$ provided that the cone is not very sharp. It can be seen from Fig. 3 that λ is smaller for smoother walls. The dependence of the optimal interface angle on β as predicted by the present model resembles the known results for plane-strain orthogonal machining (Johnson and Mellor, 1973). Also, for a smooth flat indentor, with $\beta = \pi/2$ and $m = 0$, we get a shear shock at $\lambda = 46.5$ deg which is slightly above the value of $\lambda = \pi/4$ obtained by Shield (1955) with a slip-line analysis for the flat circular smooth punch.

The criterion $\tan\gamma \rightarrow \min$ is required to compensate for lack of uniqueness in the mathematical model. The fact that the present solution predicts stronger singularities than those obtained by Fleck and Durban (1990) could reflect a better simulation of the actual elastoplastic field. A full elastic, perfectly plastic study may be needed to resolve the issue of competing near-tip singular fields in cone penetration.

The jump in shear strain at the shear shock interface is displayed in Fig. 4. The jump in $\tan\gamma$ across the shear shock

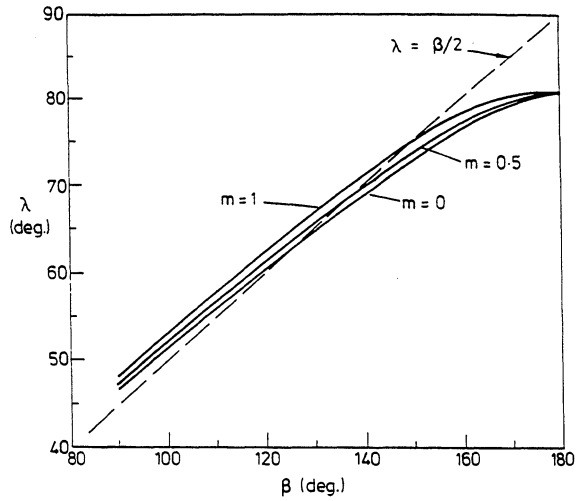

Fig. 3 Variation of optimal interface location λ with wall angle β and friction factor m

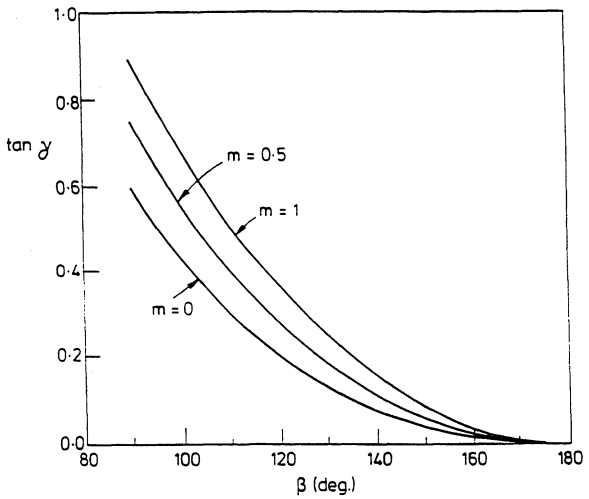

Fig. 4 Variation of shear strain tanγ at the interface with wall angle β and friction factor m

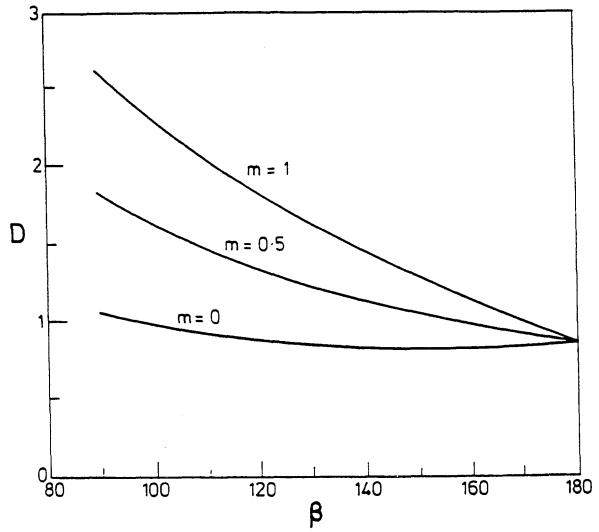

Fig. 5 Levels of stress singularity D for different wall angles β and friction factors m

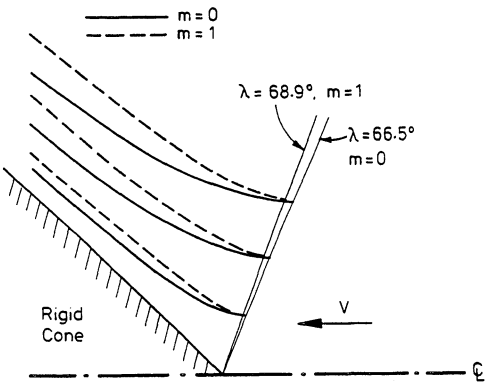

Fig. 6 Streamlines within the plastic zone. β = 135 deg.

increases with wall friction and included cone angle. The influence of m appears to decrease as β increases, though the validity of the model becomes questionable for sharp cones where the elastoplastic transition zone is likely to cover a considerable region of the flow field. This is reflected by vanishingly small values of tanγ as $\beta \to \pi$, which are not compatible with the notion of rigid/plastic discontinuity.

The stress components (24)–(26) are dominated by the logarithmic singularity of the hydrostatic stress (14). The level of that singularity is determined by constant D which is given by (29). The value of D increases with increasing m (Fig. 5) and decreases with increasing β (except for the weak minimum when $m = 0$). This behavior is physically justified since the local drag during penetration is expected to decrease for sharper and smoother cones. The values of D given in Fleck and Durban (1990) are considerably below those obtained here.

Sample calculations were performed for the shape of the streamlines in the plastic zone (Fig. 6). This is done quite easily since along a streamline $dr/r = (v_r/v_\theta)d\theta$ or, from (2)–(3),

$$r^2\phi\sin\theta = \text{constant}, \tag{43}$$

with ϕ expressed by (20).

A Particular Solution

Spencer (1984) has suggested a cone penetration model, based on the rigid/perfectly-plastic Tresca solid, with $\lambda = \pi/2$ and $\sigma_{r\theta} = 0$ everywhere within the plastic field. Thus, there are no radial shear stresses in the plastic zone, and the rigid part occupies a half space. This particular case is easily recovered from our analysis except for the difference in the value of the (Mises) yield stress k. Indeed, with $F \equiv 0$ we have from (22) that $g(\theta) \equiv 1$ and (21) admits the exact integral

$$f(\theta) = \int_{\pi/2}^{\theta} \frac{d\theta}{\sin^3\theta} = \frac{1}{2}\,\text{lntan}\,\frac{\theta}{2} - \frac{1}{2}\,\frac{\cos\theta}{\sin^2\theta}. \tag{44}$$

Equation (23) has now the simple solution $H = 2\text{lnsin}\theta + H_o$, where H_o is an integration constant, resulting in explicit r-independent expressions for the stress components (24)–(25). Likewise, the velocity components of (33) and (36) are given in terms of simple functions.

The interface shear strain (38) follows as

$$\tan\gamma = \frac{1}{\text{lntan}\,\dfrac{\beta}{2} - \dfrac{\cos\beta}{\sin^2\beta}} \tag{45}$$

predicting relatively high values of shear strain. Just to give an example, with $\beta = 135$ deg, Eq. (45) gives $\tan\gamma = 0.436$. By comparison, our model predicts for the same cone angle, with $m = 0$, an interface shear strain of $\tan\gamma = 0.096$ and an interface location of $\lambda = 66.5$ deg.

The solution (44)–(45) is valid only for a smooth cone. The stresses are nonsingular (since $D = 0$) and it is unclear whether

the jump in the shear strain (45) can exist along the interface in the absence of an active shear stress component.

Case Study: Steady Penetration by a Rod

As an application of the asymptotic analysis we shall estimate the axial force F for deep penetration of an elastic-perfectly plastic solid by a conically tipped circular rod of semi-infinite length. We assume that the rod is reduced slightly in diameter behind its conical head, so that we can neglect the effect on F of friction between the wall of the rod and of the infinite solid. However, we include the effects of friction between the head of the penetrator and the solid.

We take the conical head to be of semi-included angle $\alpha = \pi - \beta$ and of base radius a. The axial force on the penetrator F is

$$F = -\int_o^R (\sigma_{\theta\theta}(\beta)\sin\alpha + \sigma_{r\theta}(\beta)\cos\alpha)2\pi r\sin\alpha dr \qquad (46)$$

where r is the radial coordinate from the apex of the cone, and $R = a/\sin\alpha$ is the flank length of the cone. The average penetration pressure on the conical head $\bar{p} = F/\pi a^2$ is given by evaluation of (46) via (25), (26), and (28),

$$\bar{p} = -k(\sqrt{1-m^2} + H(\beta) + D\ln R) + k\left(\frac{D}{2} + m\cot\alpha\right). \qquad (47)$$

Bishop, Hill, and Mott (1945) have suggested that the penetration pressure may be estimated from the pressure required to expand a circular cylindrical cavity. We follow their suggestion and assume that the hydrostatic pressure (14) at ($r = R$, $\theta = \beta$) equals the limit pressure required to expand a cylindrical cavity in an elastic-perfectly plastic solid (Bishop et al., 1945)

$$\sigma_h(R,\beta) = k(H(\beta) + D\ln R)$$

$$= -k\left(1 + \ln\left(\frac{E}{3k}\right)\right). \qquad (48)$$

Substitution of (48) into (47) gives, using $\alpha_o = k\sqrt{3}$,

$$\frac{\bar{p}}{\sigma_o} = \frac{1}{\sqrt{3}}\left(1 + \ln\left(\frac{E}{\sigma_o\sqrt{3}}\right) + m\cot\alpha + \frac{D}{2} - \sqrt{1-m^2}\right). \qquad (49)$$

The dependence of D upon m and $\alpha = \pi - \beta$ is given in Fig. 5; thus, Eq. (49) gives in an approximate manner the effect of tip singularity, wall friction, and remote elasticity upon the penetration pressure. We note that $\bar{p}/\sigma_o$ increases with increasing E/σ_o, increasing m and decreasing α. At high values of $m \approx 1$ and large $\alpha \gtrsim \pi/4$, we expect that a false cap of nondeforming material sticks to the head of the penetrator; application of Eq. (49) then becomes inappropriate.

Table 1 Comparison of predicted penetration pressure p/σ_o with measured value for work-hardened copper, from Bishop et al. (1945). σ_o = 270 MPA, E = 124 GPA.

	$\alpha = 20^o$		$\alpha = 30^o$	
	Measured $\bar{p}/\sigma_o$	Prediction from (49)	Measured $\bar{p}/\sigma_o$	Prediction from (49)
Unlubricated (m=1)	7.4	5.7	6.8	5.2
Lubricated (m=o)	4.8	3.5	5.5	3.5

The last two terms of Eq. (49) are absent in the estimation of penetration pressure by Bishop et al. (1945). For frictionless penetration ($m = 0$), the sum of the last two terms almost vanishes for $o < \alpha < \pi/2$. For the case of sticking friction ($m = 1$), the last two terms in (49) contribute to $\bar{p}/\sigma_o$ by an amount 0.6 to 1.4, as α ranges from zero to $\pi/2$.

Bishop et al. (1945) measured the penetration pressure in annealed and in work-hardened copper using a penetrator of the type described above. A comparison of their measured penetration pressure for work hardened copper and the predictions of (49) is given in Table 1.

Equation (49) predicts qualitatively the increase in $\bar{p}/\sigma_o$ with increasing m and decreasing α, but consistently underestimates the penetration pressure by approximately 1.7 σ_o. Bishop et al. (1945) improved their estimate of $\bar{p}$ by including the effect of strain hardening in their cavity expansion calculation. The additional pressure due to strain hardening was found to equal $0.2\sigma_o$, which is negligible.

We conclude that a more complete analysis, including the effects of nonproportional loading, is required in order to obtain a more accurate solution to the penetration problem.

Acknowledgment

Part of this research was supported by Technion V.P.R. Fund—Seniel Ostrow Research Fund.

References

Bishop, R. F., Hill, R., and Mott, N. F., 1945, "The Theory of Indentation and Hardness Tests," *Proc. Physical Soc.*, Vol. 57, No. 3, pp. 147–159.

Fleck, N. A., and Durban, D., 1991, "Steady Penetration of a Rigid Cone with a Rough Wall into a Power-Law Viscous Solid," ASME JOURNAL OF APPLIED MECHANICS, Vol. 58, pp. 872–880.

Johnson, W., and Mellor, P. B., 1973, *Engineering Plasticity*, Van Nostrand Reinhold Company, London.

Lockett, F. J., 1963, "Indentation of a Rigid/Plastic Material by a Conical Indenter," *J. Mech. Phys. Solids*, Vol. 11, pp. 345–355.

Shield, R. T., 1955, "On the Plastic Flow of Metals under Conditions of Axial Symmetry," *Proc. Roy. Soc. London*, Vol. A223, pp. 267–287.

Spencer, J. M., 1984, "Plastic Flow Past a Smooth Cone," *Acta Mech.*, Vol. 54, pp. 63–74.